






Smart Glasses for Visually Evoked Potential Applications: Characterisation of the Optical Output for Different Display Technologies [†]

Alessandro Cultrera ^{1,†,*} , Pasquale Arpaia ^{2,3,4} , Luca Callegaro ¹ , Antonio Esposito ^{3,5} 
and Massimo Ortolano ^{1,5} 

¹ INRIM—Istituto Nazionale di Ricerca Metrologica, Turin, Italy; (L.C.); (M.O.)

² Department of Electrical Engineering and Information Technology (DIETI), Università degli Studi di Napoli Federico II, Naples, Italy

³ Augmented Reality for Health Monitoring Laboratory (ARHeMLab), Università degli Studi di Napoli Federico II, Naples, Italy

⁴ Centro Interdipartimentale di Ricerca in Management Sanitario e Innovazione in Sanità (CIRMIS), Università degli Studi di Napoli Federico II, Naples, Italy

⁵ Department of Electronics and Telecommunications (DET), Politecnico di Torino, Corso Duca Degli Abruzzi 24, Turin, Italy

* Correspondence: a.cultrera@inrim.it

† Presented at the 8th Electronic Conference on Sensors and Applications, 1–15 November 2021; Available online: <https://ecsa-8.sciforum.net/> (accessed date).



Citation: Cultrera, A.; Arpaia, P.; Callegaro, L.; Esposito, A.; Ortolano, M. Smart Glasses for Visually Evoked Potential Applications: Characterisation of the Optical Output for Different Display Technologies. *Eng. Proc.* **2021**, *1*, 0. <https://doi.org/>

Academic Editor: Alessandro Cultrera

Received:

Accepted:

Published: 1 November 2021

Publisher's Note: MDPI stays neutral with regard to jurisdictional claims in published maps and institutional affiliations.



Copyright: © 2021 by the authors. Licensee MDPI, Basel, Switzerland. This article is an open access article distributed under the terms and conditions of the Creative Commons Attribution (CC BY) license (<https://creativecommons.org/licenses/by/4.0/>).

Abstract: Consumer-grade available smart-glasses are being increasingly used in extended reality and brain-computer interfaces applications based on the detection of visually evoked potentials from the user's brain. The display of these kind of devices can be based on different technologies, which may affect the nature of the visual stimulus received by the user; this aspect has substantial impact in the field of applications based on wearable sensors and devices. We measured the optical output of three models of smart glasses with different display technologies using a photo-transducer, in order to get insight on their exploitability in brain-computer interfaces applications. Results suggest that preferring a particular model of smart glasses may strongly depend on the specific application requirements.

Keywords: brain-computer interface, smart glasses, optical output, visual stimulation, evoked brain potential, harmonic components.

1. Introduction

Emerging brain-computer interfaces (BCI) are being extensively investigated in the scientific community [1]. BCI provide a novel mean of communication which relies on the direct measurement of brain signals. Applications of BCI are oriented to either impaired and able-bodied people, with several already explored applications such as robots control [2], industrial inspection [3], and neurological rehabilitation [4,5]. Among various paradigms, the so-called *reactive* BCI, in which the user is exposed to a stimulus and the evoked brain response is detected, are the most performing ones [6–8]. In particular, BCI based on visually evoked potentials (VEP) are well suited for communication and control applications [3,9,10]. Visual stimulation in VEP-BCI can be performed by means of off-the-shelf smart glasses, which can generate icons of different color, shape, position and flickering rate, in the field of view of the user [3,11]. Smart glasses based on different display technologies are available on the market. Typically, smart-glasses exploit video see-through or optical see-through technology. The former consists of displaying virtual objects in superposition with a video-recording of the real environment, while the latter exploits semi-transparent displays that allows the normal vision with superimposed virtual elements [12]. Commercial devices exist which rely either on an LCD display with

an active matrix of poly-crystalline silicon thin-film-transistor, or a silicon-based OLED matrix, or even planar waveguides, among others [13]. Independently of the display technology, the visual stimuli must have some specific characteristics to be suitable for VEP-BCI applications, characteristics which may strongly depend on the smart glasses technology and implementation, first of all the ability of generating stimuli with a specific and distinguishable harmonic content. In this paper we show and discuss measurements of the optical output of smart-glasses based on three different technologies and discuss the results in terms of VEP-BCI applications.

2. Materials and Methods

Three models of commercially-available smart glasses, based on different technology, were characterised: (i) Epson BT-200 (based on LCD technology), (ii) Epson BT-350 (OLED) and (iii) Microsoft Hololens (waveguides). The smart glasses were programmed to generate, on one lens, a white rectangular icon, flickering at frequency f . To characterise the optical output of the above-mentioned smart glasses we implemented a photo-transducer (PT), schematically shown in Figure 1, based on a commercial photo-diode (OPT-101) integrated with a trans-impedance amplifier [14]. The PT was powered with a battery to avoid the line noise introduced by the mains. The micro-controller μC STM32F401RE [15] was used for the measurement of the output voltage V_{PT} of the PT and an ADC with 1 kHz sampling frequency and 12-bit resolution was used for the data acquisition to a PC. The transducer PT was placed in front of the smart glasses display with the flickering icon extending on the whole sensor area. The positioning was empirically determined by looking for the maximum measurable voltage, in each case, so that the sensor was uniformly illuminated by the icon.

In order to get meaningful results, we checked the overall bandwidth of our photo-transducer by measuring a 12 Hz square-wave optical signal generated with a LED driven by a function generator SRS DS360. The DS360 has a nominal rise time of $1.3 \mu\text{s}$ [16], while the rise time of the LED is negligible in comparison, making the test signal bandwidth large enough with respect to the PT's one (limited by the ADC). The LED resistance, equal to $1 \text{ k}\Omega$, is high enough to achieve a negligible current load for the signal generator, thus avoiding signal distortions. These preliminary measurements highlighted a discrepancy between the nominal and the measured harmonic ratios for a test square wave of less than 0.5% up to the 11th component of the measured signal V_{PT} .

The optical output of the smart glasses was recorded in a dark room for 10 s each and the considered frequency range was up to 100 Hz, which is a large enough bandwidth for VEP-BCI applications requirements, while well below the half of the sampling frequency of the ADC, in order to avoid artefacts due to aliasing.

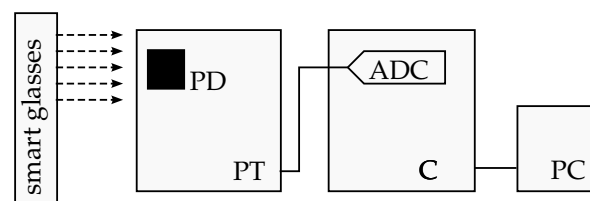


Figure 1. Schematic representation of the present experiment, with the smart glasses lens and photo-transducer PT. The dashed arrows represent the light coming from the blinking icon generated by the lens. The filled black square represents the PD sensitive area.

3. Results

Figure 2 shows the optical output, expressed as ADC voltage V_{PT} , of the three smart glasses when programmed to generate a blinking icon (a square wave visual stimulus) at $f = 10 \text{ Hz}$. The signals in time domain, Figure 2a–c are shown within a time frame of 1 s; the corresponding plots in the frequency domain in Figure 2d–f, are shown in the range up to 100 Hz. Looking at the plots in Figure 2a–c it can be seen that the three smart glasses, programmed to generate the same nominal signal, produce substantially different outputs.

In particular, the BT-200 (LCD) produce a rather symmetric wave profile, while the BT-350 (OLED) produce a strongly asymmetric profile, but in both cases the intensity changes in a smooth way; in contrast, the output of the Hololens smart glasses appears to be modulated by the repetition of fast pulses. Moreover, it can be seen that three distinct sets of pulses are present at different intensity (these are the red, green, and blue color components as verified with separate measurements).

We can consider the frequency domain, see Figure 2d–f, to get a better insight of the output harmonic content of the tested smart glasses. Again we can distinguish two cases: the BT-200 and -350 present a rather well defined harmonic content, while the Hololens does not allow to distinguish the nominal component, nor the higher components, of the test signal at frequency f . Moreover it can be noted that concerning the BT smart glasses, even though the nominal signal is a square wave, which should contain only odd-harmonics, even-harmonic components are present too (expected from the smoothing clearly visible in the time-domain plots).

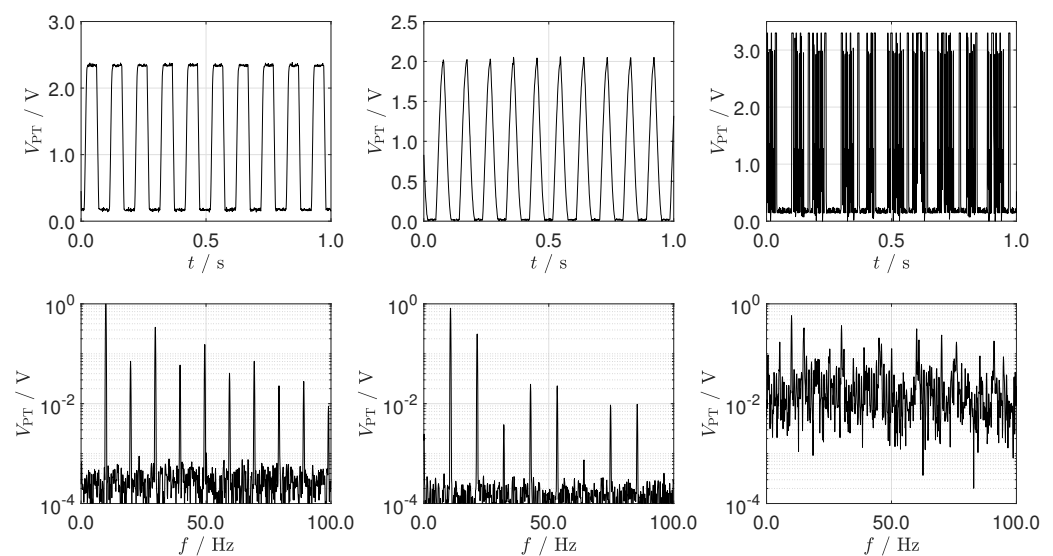


Figure 2. Optical output V_{PT} of the characterized smart glasses in the time (**above**) and frequency (**bottom**) domain. (**a,d**) BT-200, (**b,e**) BT-350, (**c,f**) Hololens.

4. Discussion

Given the present results, some considerations in terms of applicability of these off-the-shelf smart glasses to VEP-BCI can be drawn. None of the tested devices produces an optical output which is a square wave, compared to the LED-generated signal used to test the PT. In particular, even harmonics are present too in both BT-200 and BT-350 (see Figure 2d,e) and the harmonic ratios of the odd harmonics are substantially larger than 0.5% (the reference given by the test signal, see Section 3). The Hololens marks a separate case not showing any distinguishable harmonic component.

It appears that the display technology of the compared smart glasses has a strong effect on the nature of the generated visual stimulus, for the same given test waveform. This can be both related to the specific behaviour of the display matrix and also to the practical implementation of the control electronics. Note for example that the nominal refresh rate of the BT-200 is 60 Hz, while it is 30 Hz for the BT-350 and 240 Hz (with four sub-frames corresponding to an effective 60 Hz content rate) for the Hololens. It is evident from Figure 2d,f that, beside having the same effective refresh rate of 60 Hz, the BT-200 and the Hololens does not produce a similar optical output at all.

Keep in mind that these features do not imply at all costs an equivalence between the optical output and the effect of the visual stimulus on the user brain potentials. Consider that for typical VEP-BCI applications, where the evoked brain potentials of the user are

measured in order to detect the user attention oriented to a 10 Hz rather than a 12 Hz flickering icon, the distinguishability of the harmonic component can be sufficient and any additional harmonic content may be not detrimental for the task [3,5]. Moreover it can not be excluded that in terms of the net effects of the visual stimulus on the user even the HoloLens can be perfectly functional to VEP-BCI applications.

On a different ground, if these devices would be considered to study quantitative effects of visual stimuli on brain activity [17], the above-discussed features may be a stronger discriminant.

5. Conclusions

Commercial smart glasses can in principle be programmed to generate a square wave profile flickering icon, typically used as a visual stimulus in VEP-BCI applications. Anyway, the ability to generate well-separated harmonics seems to depend on the implemented the display technology. This may be not a problem in terms of sensory stimulation for the elicitation of specific brain potentials. Nevertheless, the choice of the visual stimulation technology may strongly depend on the particular target application. As a future work, it is worth studying how the different optical outputs may affect the brain potentials during VEP-BCI experiments.

Author Contributions: Conceptualization, P.A., A.C. and A.E.; methodology, all authors; software, A.E.; formal analysis, L.C, A.C., A.E. and M.O.; investigation, A.C. and A.E.; resources, P.A. and A.E.; data curation, A.C. and A.E.; writing—original draft preparation, A.C. and A.E.; writing—review and editing, all authors; visualization, A.C. and A.E.; supervision, P.A., L.C. and M.O.; project administration, P.A. and L.C.; funding acquisition, P.A. and L.C. All authors have read and agreed to the published version of the manuscript.

Funding: This research received no external funding.

Institutional Review Board Statement: XXX.

Informed Consent Statement: XXX.

Data Availability Statement: XXX.

Acknowledgments: This work was carried out as part of the “ICT for Health” project, which was financially supported by the Italian Ministry of Education, University and Research (MIUR), under the initiative ‘Departments of Excellence’ (Italian Budget Law no. 232/2016), through an excellence grant awarded to the Department of Information Technology and Electrical Engineering of the University of Naples Federico II, Naples, Italy.

Conflicts of Interest: The authors declare no conflict of interest.

References

1. Saha, S.; Mamun, K.A.; Ahmed, K.I.U.; Mostafa, R.; Naik, G.R.; Darvishi, S.; Khandoker, A.H.; Baumert, M. Progress in brain computer interface: challenges and potentials. *Front. Syst. Neurosci.* **2021**, *15*, 4.
2. Bi, L.; Fan, X.A.; Liu, Y. EEG-based brain-controlled mobile robots: A survey. *IEEE Trans. Hum.-Mach. Syst.* **2013**, *43*, 161–176.
3. Angrisani, L.; Arpaia, P.; Esposito, A.; Moccaldi, N. A wearable brain-computer interface instrument for augmented reality-based inspection in industry 4.0. *IEEE Trans. Instrum. Meas.* **2019**, *69*, 1530–1539.
4. Soekadar, S.R.; Birbaumer, N.; Slutzky, M.W.; Cohen, L.G. Brain-machine interfaces in neurorehabilitation of stroke. *Neurobiol. Dis.* **2015**, *83*, 172–179.
5. Arpaia, P.; Duraccio, L.; Moccaldi, N.; Rossi, S. Wearable brain-computer interface instrumentation for robot-based rehabilitation by augmented reality. *IEEE Trans. Instrum. Meas.* **2020**, *69*, 6362–6371.
6. Xing, X.; Wang, Y.; Pei, W.; Guo, X.; Liu, Z.; Wang, F.; Ming, G.; Zhao, H.; Gui, Q.; Chen, H. A high-speed SSVEP-based BCI using dry EEG electrodes. *Sci. Rep.* **2018**, *8*, 14708.
7. Wang, H.; Pei, Z.; Xu, L.; Xu, T.; Bezerianos, A.; Sun, Y.; Li, J. Performance enhancement of P300 detection by multiscale-CNN. *IEEE Trans. Instrum. Meas.* **2021**, *70*, 1–12.
8. Arpaia, P.; Callegaro, L.; Cultrera, A.; Esposito, A.; Ortolano, M. Metrological characterization of a low-cost electroencephalograph for wearable neural interfaces in industry 4.0 applications. In Proceedings of the 2021 IEEE International Workshop on Metrology for Industry 4.0 IoT (MetroInd4.0 IoT), Rome, Italy, 7–9 June 2021 ; pp. 1–5. <https://doi.org/10.1109/MetroInd4.0IoT51437.2021.9488445>.

9. Nguyen, T.H.; Chung, W.Y. A single-channel SSVEP-based BCI speller using deep learning. *IEEE Access* **2018**, *7*, 1752–1763.
10. Minguillon, J.; Lopez-Gordo, M.A.; Pelayo, F. Trends in EEG-BCI for daily-life: Requirements for artifact removal. *Biomed. Signal Process. Control* **2017**, *31*, 407–418.
11. Angrisani, L.; Arpaia, P.; Moccaldi, N.; Esposito, A. Wearable augmented reality and brain computer interface to improve human-robot interactions in smart industry: A feasibility study for SSVEP signals. In Proceedings of the 2018 IEEE 4th International Forum on Research and Technology for Society and Industry (RTSI), Palermo, Italy, 10–13 September 2018; pp. 1–5.
12. Chatzopoulos, D.; Bermejo, C.; Huang, Z.; Hui, P. Mobile augmented reality survey: From where we are to where we go. *IEEE Access* **2017**, *5*, 6917–6950.
13. Chen, J.; Cranton, W.; Fihn, M. *Handbook of Visual Display Technology*; Springer: Berlin/Heidelberg, Germany, 2016.
14. Texas Instruments. OPT101 Monolithic Photodiode and Single-Supply Transimpedance Amplifier (Rev. B). Available online: <https://www.ti.com/document-viewer/OPT101/datasheet/abstract#SBBS0022723> (accessed date).
15. STMicroelectronics. STM32F401xD STM32F401xE Datasheet (Rev. 3). 2015. Available online: (accessed date).
16. Stanford Research Systems. Model DS360 Ultra Low Distortion Function Generator, Operating Manual and Programming Reference. 2008. Available online: (accessed date).
17. Labecki, M.; Kus, R.; Brzozowska, A.; Stacewicz, T.; Bhattacharya, B.S.; Suffczynski, P. Nonlinear origin of ssvep spectra—A combined experimental and modeling study. *Front. Comput. Neurosci.* **2016**, *10*, 129.